

Supporting Information

Electrocatalytic Oxygen and Hydrogen Evolutions at Ni₃B/Fe₂O₃ Nanotube Arrays under Visible Light Radiation

*Hui Zhao,^a Meng Jiang,^a Qing Kang,^{*a} Lequan Liu,^b Ning Zhang,^c Pengcheng Wang,^a and Feimeng Zhou^a*

^aInstitute of Surface Analysis and Chemical Biology, University of Jinan, Jinan, Shandong 250022, P. R. China

^bTJU-NIMS International Collaboration Laboratory, Key Lab of Advanced Ceramics and Machining Technology (Ministry of Education), Tianjin Key Laboratory of Composite and Functional Materials, School of Material Science and Engineering, Tianjin University, Tianjin 300072, P. R. China.

^cSchool of Materials Science and Engineering, Central South University, Changsha, Hunan, 410083, P. R. China

*Corresponding author E-mail: ila_kangq@ujn.edu.cn

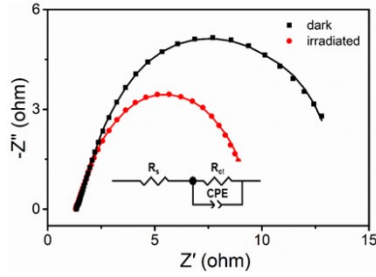


Figure S1. Nyquist plots and simulated curves of $\text{Ni}_3\text{B}/\text{Fe}_2\text{O}_3$ NTAs in dark and under one-sun radiation. The equivalent circuit is shown with the solution resistance denoted as R_s , the charge transfer resistor as R_{ct} and the constant-phase element as CPE.

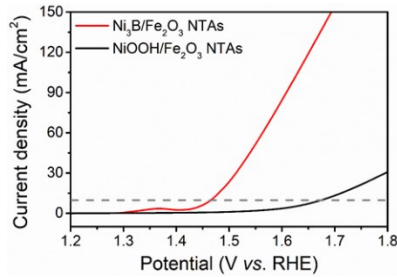


Figure S2. OER polarization curves of $\text{Ni}_3\text{B}/\text{Fe}_2\text{O}_3$ NTAs and $\text{NiOOH}/\text{Fe}_2\text{O}_3$ NTAs under one-sun radiation.

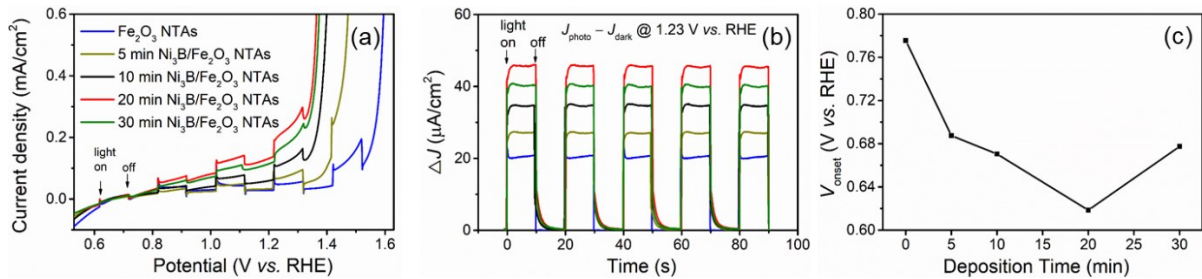


Figure S3. OER (a) polarization curves and (b) chronoamperograms at 1.23 V at the bare Fe_2O_3 NTAs and Fe_2O_3 NTAs modified with Ni_3B using different deposition times (5, 10, 20, and 30 min) under repeated on-off radiation sequences. (c) The onset potential plotted vs. deposition time.

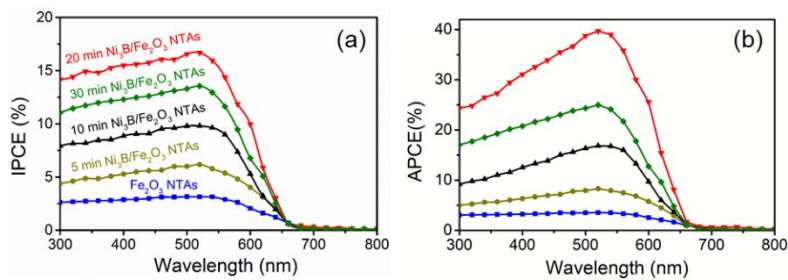


Figure S4. IPCE and APCE spectra at 1.23 V of bare Fe_2O_3 NTAs and Fe_2O_3 NTAs modified with Ni_3B using different deposition times (5, 10, 20, and 30 min).

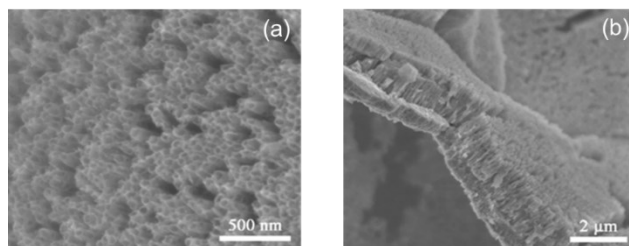


Figure S5. Field emission-SEM images of the top (a) and cross section (b) of Fe_2O_3 NTAs.

In Figure S5, the Fe_2O_3 NTAs have an average inner diameter of 55 nm and a length of 2.05 μm . The vertically oriented and aligned NTAs promote the directional charge transport due to the one-dimensionality of the tubes.¹

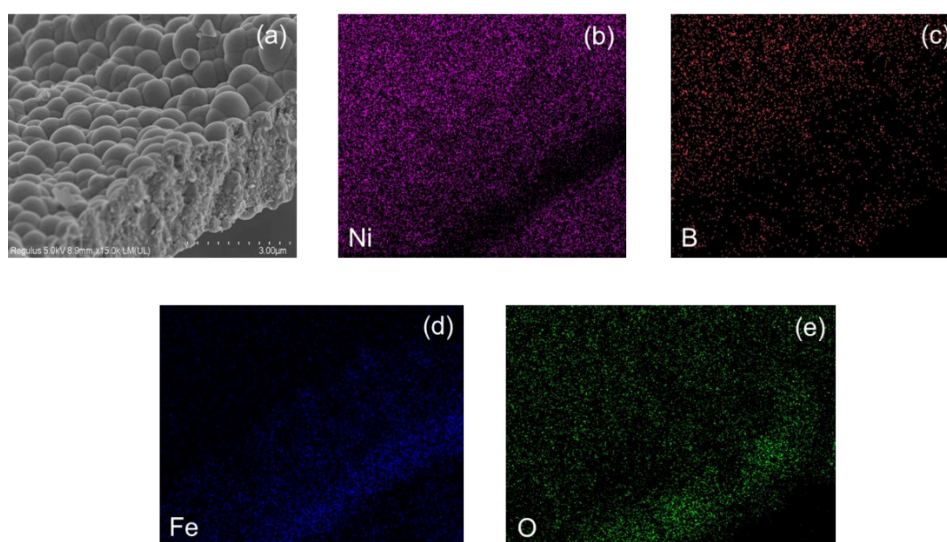


Figure S6. A field emission-SEM image (a) of the $\text{Ni}_3\text{B}/\text{Fe}_2\text{O}_3$ NTAs and the energy dispersive X-ray spectroscopic (EDS) maps corresponding to Ni (b), B (c), Fe (d), and O (e).

Figure S6a is a field emission-SEM image of the cross section of a $\text{Ni}_3\text{B}/\text{Fe}_2\text{O}_3$ NTA, revealing that the nanotubes have an average thickness of 2.25 μm . The thickness of the Ni_3B layer was determined to be around 0.20 μm from the SEM and EDS elemental mapping analysis (Figure S6b-e).

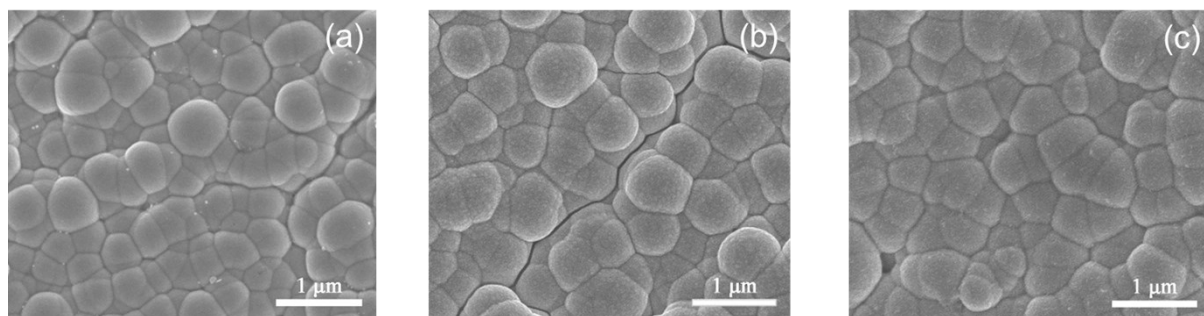


Figure S7. SEM images of $\text{Ni}_3\text{B}/\text{Fe}_2\text{O}_3$ NTAs before (a) and after OER (b) and HER (c).

A field emission-SEM image of a Ni₃B/Fe₂O₃ NTAs (Figure S7a) shows that the entire surface of the Fe foil was uniformly covered with Fe₂O₃ NTAs. After OER, the surface of the Ni₃B/Fe₂O₃ NTAs became rougher and contained numerous nanoparticles (Figure S7b). A closer examination reveals that the nanoparticles are 40 ± 10 nm in diameter. Such a morphological change is likely originated from the Ni₃B oxidation.^{2, 3} After HER in alkaline solution, some small burr-like structures covered the Ni₃B/Fe₂O₃ NTAs (Figure S7c).

Table S1. Calculated values of the solution resistor (R_s), charge transfer resistor (R_{ct}) and constant phase element (CPE) on the fitted equivalent circuit of Ni₃B/Fe₂O₃ NTAs in dark and under one-sun radiation.

Condition	R_s (Ω)	R_{ct} (Ω)	CPE (mF/cm ²)
Under irradiation	1.33	8.44	34.93
In dark	1.36	13.17	33.56

Table S2. Best fitted parameters of time-resolved photoluminescence.

Samples	Decay lifetimes (ns)			Fractional contribution			Average lifetimes (τ_{Avg} , ns)
	τ_1	τ_2	τ_3	f_1	f_2	f_3	
Fe ₂ O ₃ NTAs	7.50	55.54	1.33	0.14	0.04	0.82	4.36
Ni ₃ B/Fe ₂ O ₃ NTAs	7.79	48.05	1.55	0.14	0.04	0.82	4.28

Reference

1. T. J. LaTempa, X. Feng, M. Paulose and C. A. Grimes, *J. Phys. Chem. C*, 2009, **113**, 16293–16298.
2. H. Li, P. Wen, Q. Li, C. Dun, J. Xing, C. Lu, S. Adhikari, L. Jiang, D. L. Carroll and S. M. Geyer, *Adv. Energy Mater.*, 2017, **7**, 1700513.
3. Z. Chen, Q. Kang, G. Cao, N. Xu, H. Dai and P. Wang, *Int. J. Hydrogen Energ.*, 2018, **43**, 6076–6087.